Bachelor Thesis

Institut für Physik

Impact of the gap morphology on the optical properties of plasmonic nanoparticles

Advisor:

Ao. Univ. Prof. Dr. Ulrich Hohenester

Benedikt Gasplmayr

Mat.Nr. 01530104

Wintersemester 2019

1. Abstract

The focus in this theses was to take a look at the resonance frequency of two coupled gold rods with either spherical or rectangular caps. The resonance frequency was calculated for varying distances between the rods.
Furthermore, the resulting surface charge was expanded into eigenmodes and the expansion coefficients were calculated. This was done with MATLAB and MNPBEM toolbox.
In the first step, the rods separated by some distance , were excited with a plane wave. The resulting fields were calculated by solving Maxwells' equations using the toolbox. This was repeated for various distances. From these, the resonance frequency could be determined.
The same procedure was used to get the expansion coefficients when expanding the surface charge into the eigenmodes at various distances. The result for the resonance frequency showed a red shift with decreasing distance. The rod with rectangular cap showed a smaller wavelength at larger distances but was subject to a steeper increase when the distance decreased. This behaviour can also be seen in [3].
In the expansion, the dipole mode was the most dominant order in both cases.
In a logarithmic plot of the coefficient's modulus the red-shift was also present.

Inhaltsverzeichnis

1. Abstract **2**

2. Introduction **4**
2.1. Basic Concepts 4
2.2. Light matter electronic interaction in nano-gaps 5
2.3. Plasmon-Phonon Coupling 6
2.4. Conduction and bridging in nano-gaps 6
2.5. Future applications 6
2.6. In this Thesis 7

3. Theory **8**
3.1. Wave equation in quasistatic limit 8
3.2. Green's functions 9
3.3. Boundary integral method 10
3.4. Plasmonic coupling 11
3.5. Scattering cross-section 11

4. MNPBEM toolbox **13**

5. Code description and system simulated **14**

6. Results **18**
6.1. Redshift of resonance frequency 18
6.2. Expansion coefficients 19

7. Summary **21**
7.1. Distance variation of the Rods 21
7.2. Calculating the expansion coefficients 21

A. Code for finding resonance frequencies (spherical caps) **22**

B. Code for finding resonance frequencies (rectangular caps) **25**

C. Calculating coefficients for rectangular rods **27**

D. Calculating coefficients for spherical rods **29**

2. Introduction

Plasmons are excitations of metallic nano particles embedded in a dielectric material. Plasmonic properties highly depend on shape, form and material properties and can therefore be manipulated in many ways.
Plasmonics rapidly gained attention in the 1990's when local fields around nano-structures could be measured for the first time.
By using those nano-structures it is possible to confine light. The scale of this confinement is usually far smaller than the free-space wavelength. E.g in some cases it was possible to localize light with copper, gold, silver or aluminium nano-particles with sharp edges in volumes. The minimum dimensions were around 10-100 nm. Reaching smaller distances is possible but the implementation with a single particle is very difficult due to technical limitations, e.g fabrication. For some applications like surface-enhanced Raman scattering (SERS) it is necessary to archive a high and tight field strength.
Using coupled nano-particles is an alternative Ansatz to using single rods. Light can be localised in the gap between them but here the same limitations are present.
A different approach is to use so called nano antennas. Two metal layers are separated by a dielectric. A so called gap plasmon is embedded in this dielectric. The advantage of this lies in the ease of production combined with extreme field enhancement and sensitivity with regards to single atom placements. In fact, nano-optical antennas are part of the 'extreme nano-optics'. [1, S. 668]

2.1. Basic Concepts

For a metal-insulator-metal multilayer, the dispersion relation is given through [2]

$$(k_{\parallel}/k_0)^2 = n_{eff}^2 = \epsilon_g + 2\zeta[1 + \sqrt{1 + (\epsilon_g - \epsilon_m)/\zeta}] \tag{1}$$

with ϵ_g being the permittivity of the dielectric gap, ϵ_m being the permittivity of the metal layers and

$$\zeta = (k_0 \cdot d \cdot \epsilon_m/\epsilon_g)^{-2} \tag{2}$$

This relationship is valid for gap distances $d < 10$ nm.
The facets of a particle, figure 1 left, break this continuum into discrete modes and localizes them in the small gap. The discrete wavelengths are

$$\lambda_i^s \simeq \lambda_p \sqrt{\frac{w\epsilon_g}{d\ \alpha_i} + \epsilon_\infty} \tag{3}$$

with w being the facet length of the particle, α_i the roots of the Bessel function, λ_p being the plasma frequency, ϵ_∞ being the dielectric background and a Drude-metal permittivity of $\epsilon_m = \epsilon_\infty - \lambda^2/\lambda_p^2$ is used. By varying w the whole visible and infra-red spectrum can be covered. However these modes couple poorly with free space.

But they couple easily with plasmonic antenna modes. By using simple LCR circuits and a quasi static field response, the first antenna mode yields

$$\lambda^{(1)} = \lambda_p \sqrt{\epsilon_\infty + 2\epsilon_d + 4\epsilon_d C_g / C_{NP}} \tag{4}$$

with C_d being the capacitance of the gap, $C_{NP}$the capacitance of the nano-particle and ϵ_d the permittivity of the gap. If one considers a spherical nano-particle with $C_{NP} = C_g \epsilon_g^\chi \ \ln(1 + \zeta R/d)$, $\chi \approx 0.5, \zeta \approx 0.5$, this results in

$$(\lambda^{(1)}/\lambda_p)^2 = \epsilon_\infty + 2\epsilon_d + 4\epsilon_g^\chi \ \ln(1 + \zeta R/d) \tag{5}$$

Equation (5) results in a red-shift if the gap distance d decreases. Such antenna-nano gap plasmons depend highly on the shape of the facets. [1, S. 669]

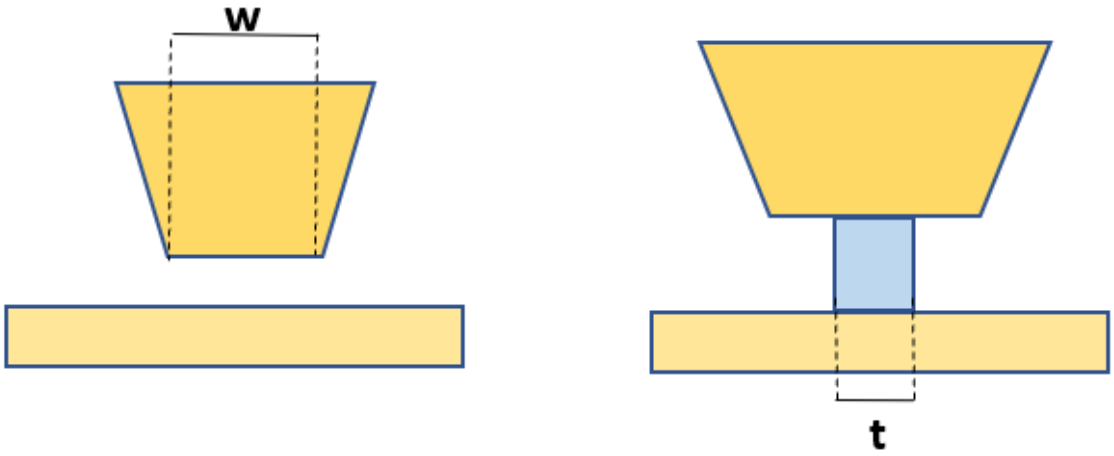

Figure 1: Metallic facet with (right) and without (left) a conducting spacer.

2.2. Light matter electronic interaction in nano-gaps

Emitters experience modified absorption and emission rates when placed in the enhanced field inside the gap which can lead to strong coupling. To achieve this, the orientation of the emitter's position and dipole are important. The field in the gap can vary strongly within nano-meters which makes this strong coupling difficult.
Interestingly, concerning fluoresce properties, enhancement, reduction and quenching has been observed. These depend on position, geometry and dimension of the gap. The changes can be explained on a quantum level by quantum yields and altered efficiencies of excitation. Quantum yields are the probability that excitation results in a photon
The strong dependency on position allows tailoring the spontaneous emission rate to build ultra-fast low power light sources, modulators and single photon emitters. [1, S. 671]

2.3. Plasmon-Phonon Coupling

The extreme surface enhanced Raman signal (SERS), which is a surface sensitive Raman spectroscopy, enables a localized detection of ultra-thin materials. A robust and accurate SERS signal is needed to exactly identify materials. These signals however can vary from structure to structure. A solution are gap plasmons when the optimal field distribution, enhancements and dipole orientation are precisely known. [1, S. 671-672]

2.4. Conduction and bridging in nano-gaps

It is also possible to consider a conducting spacer in the nano-gap. These spacers can be described with the model of a perturbed Fabry-Perot metal-insulator-metal layer, which has a facet length w and a conducting layer of width t (figure 1 right). This defines a perturbed cavity length $L_g = (w - t)/2$. The resonance condition becomes

$$L_g = r'\lambda_r/2 \tag{6}$$

$r' = r + \phi_g/2\pi$, $r = 0, 1, 2...$ is the so called groove cavity mode and $\phi_g \sim \pi/2$ is the resonance condition at the boundaries. The dispersion relation is the same as equation 1 with a modified groove wave vector $k_r = 2\pi/\lambda_r$.
As in section 2.1, one can couple these modes to antenna modes which causes radiation. At a wavelength near 700 nm these modes are barely perturbed by the bridging. Additionally, the near field decays exponentially in the bridge. A wider bridge causes the confined modes to blue-shift because of a smaller L_g. Such conductive bridges are studied to build resistive- RAM devices. These are non-volatile and low energy storage devices. [1, S. 673]

2.5. Future applications

Several techniques allow precise coating. By using them it is possible to create meta-surfaces. These surfaces allow to tailor the electric and magnetic properties of a material by exploiting plasmonic effects.
By matching the gap length to the diameter of the plasmonic particle, it is possible to achieve near perfect absorption at the plasmon resonance length. This can be useful for hot-electron photo-detectors, thermal detectors and light harvesting.
In general, the high dependence on a material's properties gives potential for sensitive sensors or switching.
The field of extreme nano-optics allows for chemical reactions and functional surface electro-chemistry to be studied at molecular scale. Also electrochemical processes can be studied better by using SERS and scattering during reactions. The difficulty, however, is that there is not yet a market for this application which limits the scientific research in this field.
Furthermore, the tune-ability of plasmon modes and electronic states allows for a better studying of electrochemical reaction.
However quantitative information is missing here. As mentioned in section 2.2 it is

possible to tailor the spontaneous emission rate of emitters in the nano-gap to build ultra-fast optical applications [1, S. 675-676]

2.6. In this Thesis

In this thesis 2 golden nano-particles are consider. They are excited by light (400 nm -900 nm). As mentioned in 2.1, the resonance wavelength should redshift if the gap distance decreases. The resulting surface charge will then be numerically expanded into its eigenmodes and the expansion coefficients calculated.

3. Theory

An electromagnetic wave hitting a metal causes some interesting physics to happen on the interface between the metal and the surrounding dielectric. The system considered in this thesis consists of two metallic (golden) nano-rods that are excited by an incident light wave. This results in an surface charge oscillation whose amplitude depends on the excitation wavelength. These surface charge oscillations can be expanded into eigenmodes. In this section, at first the physics for spherical metallic particles being excited is discussed. Afterwards, Green's functions are shortly introduced to extend the approach in section 3.1 to arbitrary geometries. Finally, plasmonic coupling and the important quantities for scattering are shortly introduced.

3.1. Wave equation in quasistatic limit

The wave equation for the scalar potential

$$(\nabla^2 + k^2)V(\mathbf{r}) = -\frac{\rho(\mathbf{r})}{\epsilon} \tag{7}$$

with $k^2 = \epsilon\mu\omega^2$ is the starting point for this consideration. It can be derived by working in the Lorenz gauge condition

$$\boldsymbol{\nabla} \cdot \mathbf{A} = i\sqrt{\mu\epsilon}kV(\mathbf{r}) \tag{8}$$

The characteristic wavelength of the exciting wave, λ, is much larger than the characteristic length scale of the nano particle L. The Laplace operator gives the curvature of the function. With this, following approximation can be done

$$|\nabla^2 V| \sim \frac{1}{L^2}|V| \gg \frac{1}{\lambda^2}|V| \sim k^2|V| \tag{9}$$

Which justifies dropping the $k^2V(\mathbf{r})$ term in the wave equation. For further simplification consider the Lorenz gauge condition

$$L|\boldsymbol{\nabla} \cdot \mathbf{A}| = L|i\sqrt{\mu\epsilon}kV(\mathbf{r})| \sim \frac{L}{\lambda}|V| \ll |V| \tag{10}$$

This approximation tells that the absolute value of the vector potential is much smaller than the scalar potential and therefore can be neglected and using $\mathbf{E}(\mathbf{r}) = -\boldsymbol{\nabla}V(\mathbf{r})$ is justified. Finally, the dielectric permeability is assigned a frequency dependency which leads to the quasi-static approximation

$$\nabla^2 V(\mathbf{r}) = -\frac{\rho(\mathbf{r})}{\epsilon(\omega)} \tag{11}$$

This approximation is valid if the wavelength is much larger than the size of the nanoparticle. The goal is to solve Maxwell's equations in the quasistatic approximation for

spherical particles, obtain the surface charge and then go to numerical methods for more difficult geometries.

Consider an electric field polarized along the $\hat{\mathbf{z}}$ axis of the form

$$V(\mathbf{r}) = -E_0 \hat{\mathbf{z}} \cdot \mathbf{r} \tag{12}$$

exciting a sphere with radius a. In spherical coordinates (11) does not depend on the azimuthal angle and can therefore be solved with the Ansatz

$$V(r,\theta) = \sum_{l=0}^{\infty} \left(A_l r^l + \frac{B_l}{r^{l+1}} \right) P_l(\cos\theta) \tag{13}$$

with P_l being the Legendre polynomials, which leads to the result

$$V(r,\theta) = \begin{cases} -\left(\frac{3\epsilon_{out}}{\epsilon_{in}+2\epsilon_{out}}\right) E_0 r\cos\theta, & \text{for } r \leq a \\ \left(\frac{\epsilon_{in}-\epsilon_{out}}{\epsilon_{in}+2\epsilon_{out}}\right) \frac{a^3}{r^2} E_0 r\cos\theta - rE_0\cos\theta, & \text{for } r > a \end{cases} \tag{14}$$

with the boundary conditions

- $(V_{out} - V_{in})|_{r=a} = 0$
- $V \to -zE_0 r \quad$ for large r
- $(\epsilon_{in}\frac{\partial V_{in}}{\partial r})_{r=a} = (\epsilon_{out}\frac{\partial V_{out}}{\partial r})_{r=a}$

The first term of the potential outside is an induced part with the form of a dipole only relevant close to the sphere with a dipole moment

$$\mathbf{p} = 4\pi\epsilon_{out} \left(\frac{\epsilon_{in} - \epsilon_{out}}{\epsilon_{in} + 2\epsilon_{out}} \right) a^3 E_0 \hat{\mathbf{z}} \tag{15}$$

The surface charge can be calculated from (14) with

$$\sigma_{pol} = -\epsilon_0 (E^{\perp}_{out} - E^{\perp}_{in}) = 3\epsilon_0 \left(\frac{\epsilon_{in} - \epsilon_{out}}{\epsilon_{in} + 2\epsilon_{out}} \right) \tag{16}$$

For metallic materials $\epsilon_{in}(\omega)$ can become negative below the plasma-frequency which can result in very large surface charges. Such excitations are called particle plasmons. They usually have a very high amplitude with one resonance frequency and are confined to the sphere. [4, S. 123-130]

3.2. Green's functions

Green's functions are a very useful tool to solve differential equations. A Green function is defined as

$$L(\mathbf{r})G(\mathbf{r},\mathbf{r}_0) = -\delta(\mathbf{r} - \mathbf{r}_0) \tag{17}$$

where $L(\mathbf{r})$ is a linear differential operator. Green's functions are defined such that they are solving equations of the form

$$L(\mathbf{r})f(\mathbf{r}) = -s(\mathbf{r}) \tag{18}$$

The solution $f(\mathbf{r})$ can be obtained by

$$f(\mathbf{r}) = \int G(\mathbf{r}, \mathbf{r}')\ s(\mathbf{r}')\ d^3r' \tag{19}$$

The proper boundary conditions need to be built into a Green function. Green functions are extremely useful for solving linear differential equations (for example Maxwell's equations) and can physically be interpreted as the response of system to a point like source. [4, S. 67-79]

3.3. Boundary integral method

To compute the surface charge for arbitrary geometries other methods are needed. One of these is the boundary integral method. Here the potential is written as a sum of the potential inside, $V_{inc}(\mathbf{r})$, and on the boundary of the particle

$$V(\mathbf{r}) = V_{inc}(\mathbf{r}) + \oint_{\partial S} G(\mathbf{r}, \mathbf{s})\sigma(\mathbf{s})dS \tag{20}$$

with $G(\mathbf{r}, \mathbf{s})$ being the Green function for the Poisson equation

$$G(\mathbf{r}, \mathbf{s}) = \frac{1}{4\pi|\mathbf{r} - \mathbf{s}|} \tag{21}$$

$\mathbf{r}$ is position inside the sphere and $\mathbf{s}$ is a position on the surface S. The surface charge can be calculated by using the boundary conditions via the Dirichlet and Von Neumann trace. The result for the surface charge is

$$\Lambda(\omega)\sigma(\mathbf{s}) + \oint_{\partial S} \frac{\partial G(\mathbf{s}, \mathbf{s}')}{\partial n} dS' = -\frac{\partial V_{inc}(\mathbf{s})}{\partial n} \tag{22}$$

with $\partial/\partial n$ being the normal derivative. One big advantage of (22) is that it can be solved by expanding $\sigma(\mathbf{s})$ into eigenmodes

$$\sigma(\mathbf{s}) = \sum_k c_k u_k(\mathbf{s}) \tag{23}$$

The eigenvalue equation for equation (23) reads

$$\oint_{\partial\Omega} \frac{\partial G(\mathbf{s}, \mathbf{s}')}{\partial n} u_k(\mathbf{s}')dS' = \lambda_k u_k \tag{24}$$

$$\oint_{\partial\Omega} \tilde{u}_k(\mathbf{s}') \frac{\partial G(\mathbf{s}', \mathbf{s})}{\partial n} dS' = \lambda_k \tilde{u}_k \tag{25}$$

with u_k being the right and $\tilde{u}_k$ being the left eigenvectors. In terms of these eigenvectors equation (22) can be solved in the form

$$\sigma(\mathbf{s}) = -\sum_k (\Lambda(\omega) + \lambda_k)^{-1} \left[\oint_{\partial S} \tilde{u}_k(\mathbf{s}) \frac{\partial V_{inc}(\mathbf{s}')}{\partial n'} dS' \right] u_k(\mathbf{s}) \tag{26}$$

An exact derivation is given in [4, S. 135-140]

3.4. Plasmonic coupling

For plasmonic particles that are close enough together, the induced electric field in the rod results in a coupling with another rod to minimize the systems energy. This coupling can be described analogous to the molecular orbital theory. The system is described by a surface charge $\sigma(\mathbf{r})$ which can , like in molecular orbital theory, be expressed as a linear combination

$$\sigma(\mathbf{r}) = \sum_i c_i \tilde{\psi}_i \tag{27}$$

$\tilde{\psi}_i$ are the eigenstates or eigenmodes of the of the constituent particles. Like in molecular orbital theory, the $\tilde{\psi}_i$ either are binding (symmetric) or anti-binding (antisymmetric) modes.

As mentioned in 2.1, plasmonic coupling leads to strong enhanced electric fields in the gap and the excitation frequency redshifts if the distance decreases.

3.5. Scattering cross-section

The general form of an induced dipole moment induced by an incoming electric field $\mathbf{E}_{inc}$ is

$$\mathbf{p} = \bar{\bar{a}}(\omega) \cdot \mathbf{E}_{inc} \tag{28}$$

with $\bar{\bar{a}}(\omega)$ being the frequency dependent polarizability, a second rank tensor.

The general expression for the scattered Power of an rotating dipole is

$$P_{sca} = \frac{1}{2} \oint_{\partial\Omega} \mathrm{Re}(\ \mathbf{E}_{sca} \times \mathbf{H}^*_{sca}) \cdot \hat{\mathbf{r}}\ dS \tag{29}$$

Inserting the electric, $\mathbf{E}_{sca}$, and magnetic field, $\mathbf{H}_{sca}$, for an oscillating dipole in the far field approximation ($kr << 1$)

$$\mathbf{E}_{sca} = \frac{e^{ikr}}{r} \frac{k^2}{4\pi\epsilon_0} \mathbf{p}_\perp \tag{30}$$

$$\mathbf{H}_{sca} = Z^{-1} \frac{e^{ikr}}{r} \frac{k^2}{4\pi\epsilon_0} \mathbf{r} \times \mathbf{p}_\perp \tag{31}$$

$$\mathbf{p}_\perp = \mathbf{p} - \hat{\mathbf{r}}(\hat{\mathbf{r}} \cdot \mathbf{p}) \tag{32}$$

yields

$$P_{sca} = Z^{-1} \frac{k^4 p^2}{12\pi\epsilon_0^2} \tag{33}$$

Dividing this through the intensity of the incident wave $\frac{1}{2} Z^{-1} |E_0|^2$ results in the scattering cross section of a polarizable particle

$$C_{sca} = \frac{k^4}{6\pi\epsilon_0} |\bar{\bar{a}} \cdot \epsilon_0|^2 \tag{34}$$

$\bar{\bar{a}}$ is the polarization tensor of the particle. C_{sca} describes the scattering cross-section of a particle hit by an incident wave of the form $E_0\epsilon_{\mathbf{0}}$. [4, S. 132-133]

4. MNPBEM toolbox

The MNPBEM(metallic nanoparticles boundary element method) is a MATLAB-toolbox used for simulating the behaviour of metallic nanoparticles embedded in a dielectric environment. This is done by solving Maxwell's equations with appropriate boundary conditions. The method works best for metallic nanoparticles with scales around a few nanometres to a few hundred nanometres. The following steps are necessary in each simulation [5]

- define the dielectric functions
- define particle boundaries
- specify how particle is embedded in dielectric environment
- set up solver for the BEM equations
- specify the excitation scheme
- solve the BEM equations for the given excitation by computing the axillary surface charges
- compute the response of the plasmonic nanoparticle for the given excitations

5. Code description and system simulated

Th system to be simulated consists od two rods with either two rods made out of gold with spherical and rectangular caps as shown in Figure 2 and 3 in a vacuum environment excited with light in $\hat{z}$-direction.

Figure 2: Rods with spherical caps

For the initialisation a few commands are important.

```
op = bemoptions(op, PropertyName, PropertyValue)
```

sets the standard options for the simulations

```
exc = planewave( pol, op, PropertyName, PropertyValue)
```

initialises the planewave-excitation with polarisation pol and options op set by the command *bemoptions*.

After this, a loop follows which iterates over all wavelengths in

```
enei = linspace( 400, 900, 1000)
```

Figure 3: Rods with rectangular caps

During each step of the loop the folllowing has the be done:

```
p = trirod( diameter, height, [ nphi, ntheta, nz ] );
```

creates a discretized spherical rod. To eventually get the system of two rods

```
p1 = shift( p, [ 0, 0, -0.5 * ( height + gap(n) ) ] );
p1 = shift( p, [ 0, 0,  0.5 * ( height + gap(n) ) ] );
```

is used to shift the rods in the z-axis. This has to be done at each step of the loop.

```
pp = comparticles( varargin )
```

takes the input and and initialises a compound system with specifications as given through *varargin*.

```
sig = bem( varargin )
```

solves Maxwell's equations specified with *varargin*.

With the solutions of Maxwell's equations the scattering cross-section can be calculated and the biggest value is stored in a preallocated array.

The increase precision and save time

```
spline( varargin )
```

is used.

An example of a spectrum for the wavelength of 900 nm and gap distance 25 nm is in Figure 4 and a pseudo-code is in Figure 5

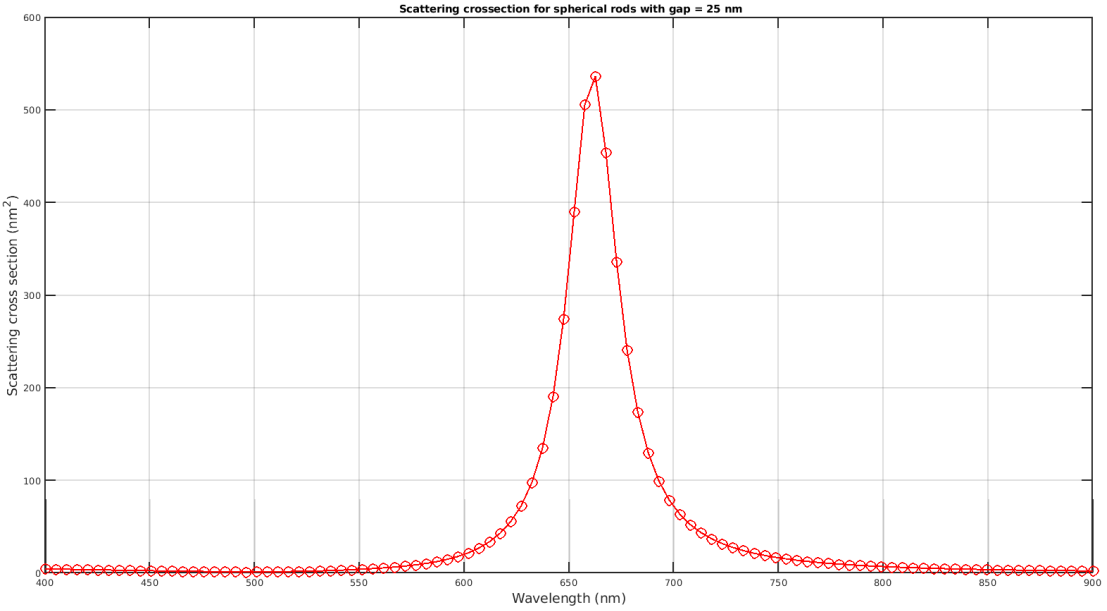

Figure 4: Example spectrum for $\lambda = 900$ nm and gap distance 25 nm

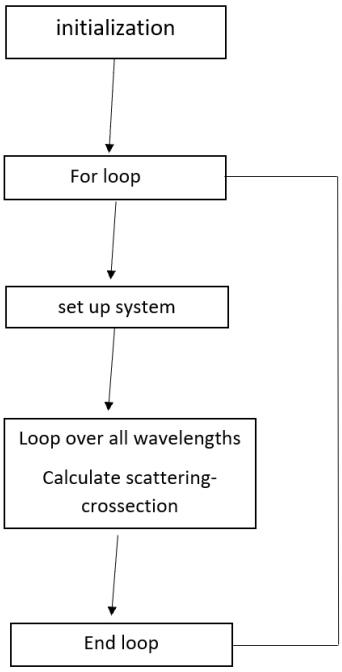

Figure 5: Pseudo-code for calculating the resonance frequency

This is done analogues for spherical and rectangular caps.

The expansion coefficients in

$$\sigma = \sum_i c_i u_i$$

are calculated in a different script (Appendix C and Appendix D). Here, again, this is done analogues for spherical and rectangular caps and at the beginning is the same initialization as above. The only difference is a loop (line 68-72) over the number of eigenvalues (nev) according to

$$\sigma(\mathbf{s}) = -\sum_k (\Lambda(\omega) + \lambda_k)^{-1} \left[\oint_{\partial S} \tilde{u}_k(\mathbf{s}) \frac{\partial V_{inc}(\mathbf{s}')}{\partial n'} dS' \right] u_k(\mathbf{s})$$

The left eigenvectors are obtained by (line 56)

```
[~, ~, ul ] = plasmonmode( pp, nev );
```

In Figure 6 is a pseudo-code for the calculation of the coefficients

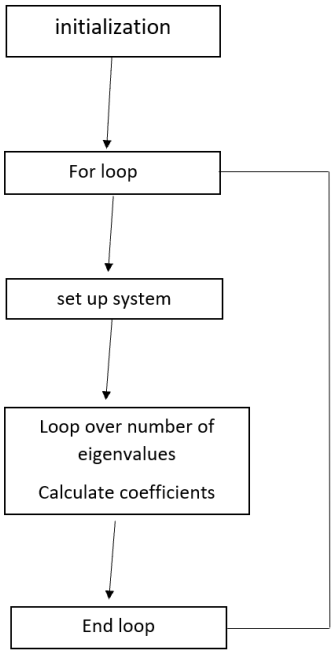

Figure 6: Pseudo-code for calculating the expansion coefficients

6. Results

6.1. Redshift of resonance frequency

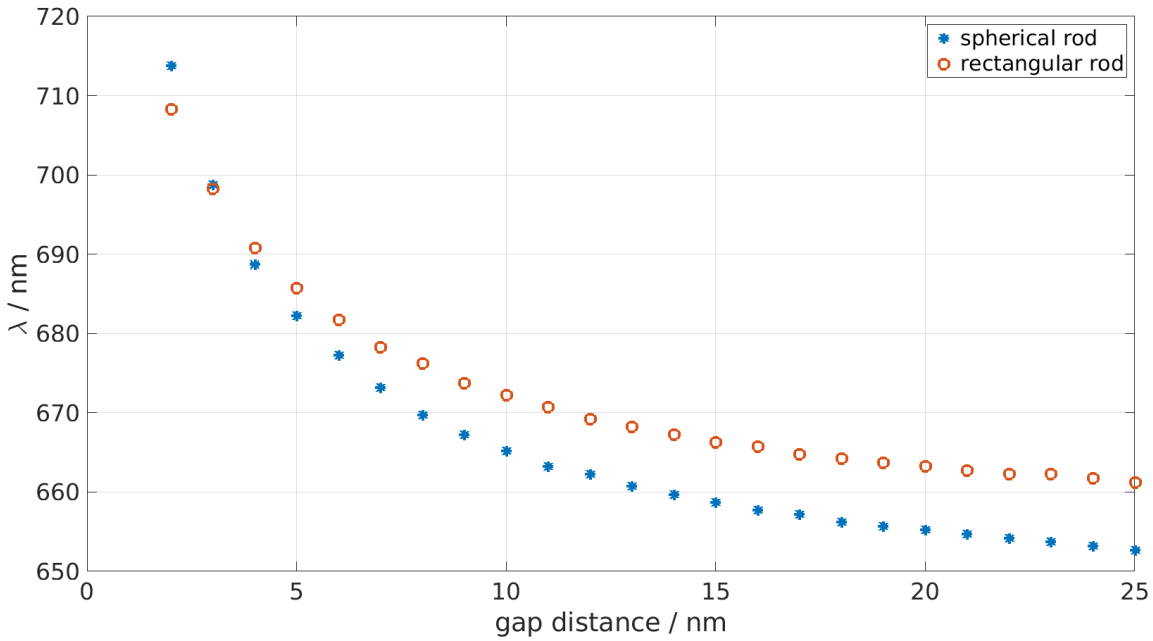

Figure 7: Resonance wavelength vs distance

In Figure 7 the change of the resonance frequency of the two rod system with gap distance is shown. It can be clearly seen that the resonance wavelength is subject to a redshift as the distance decreases. This behaviour can also be seen in [3]. Depicting smaller distances is not possible since quantum effects become relevant that are not considered in the MNPBEM toolbox.

6.2. Expansion coefficients

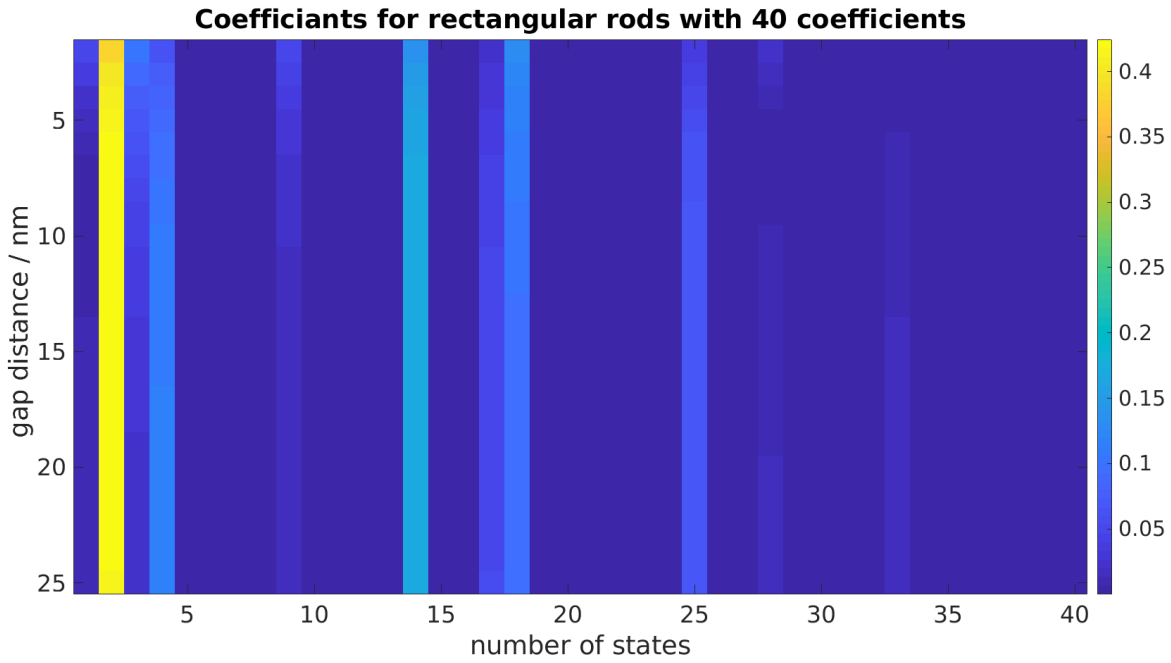

Figure 8: Coefficients for rectangular rods as function of gap distance and number of coefficients

In Figure 8 and Figure 9 the coefficients of the expansion

$$\sigma(\mathbf{s}) = \sum_n c_n u_n$$

for one spherical and one rectangular rod are depicted. Both rods show a similar behaviour the dipole and quadrupole moment are present in both cases and only vary in magnitude. Differences can be seen in higher modes which is probably due to the geometry. This results in a different surface charge and thus a different coupling.

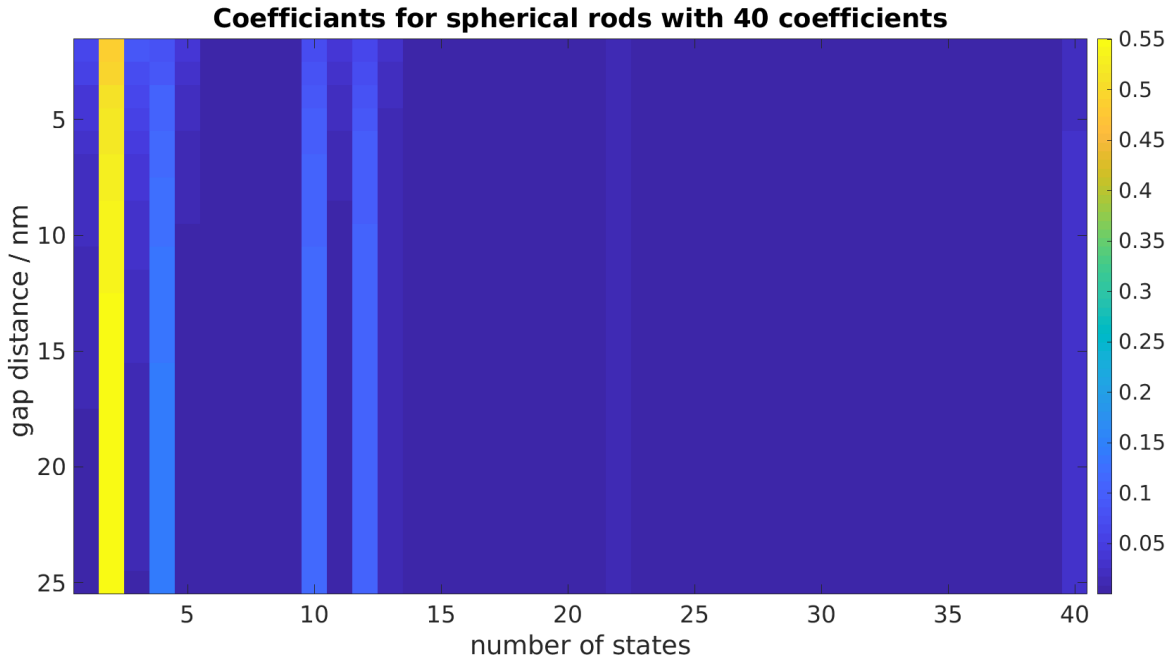

Figure 9: Coefficients for spherical rods as function of gap distance and number of coefficients

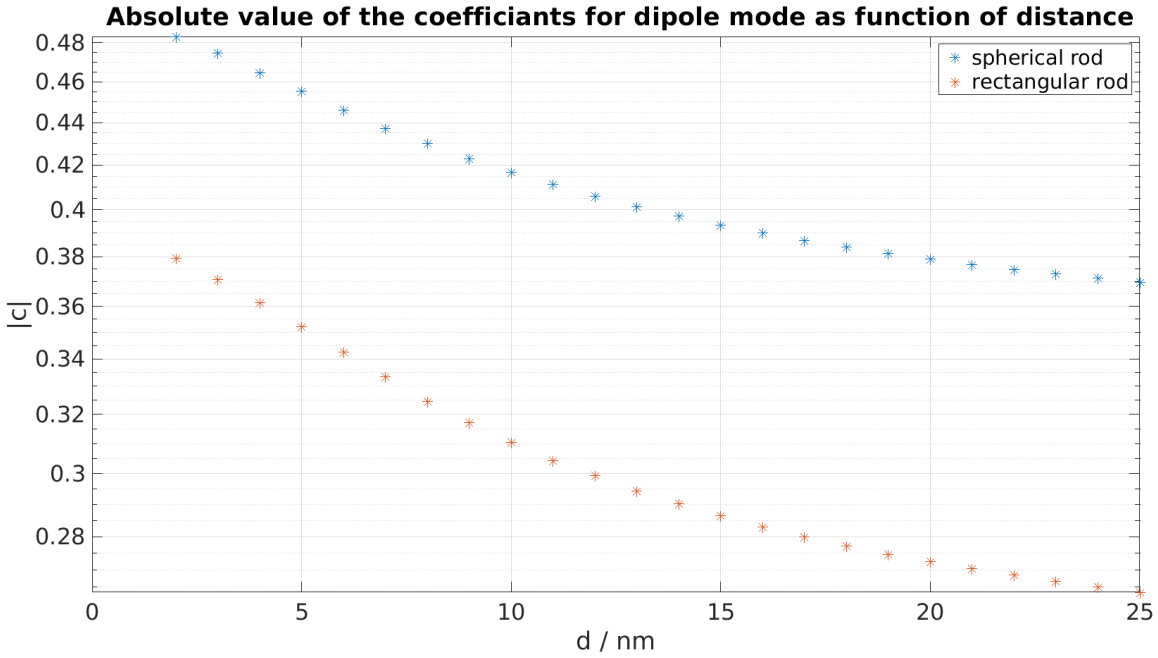

Figure 10: Dipole coefficients for spherical and rectangular rods as function of gap distance

Figure 10 shows the absolute value of the expansion coefficients for the dipole mode as a function of distance.

7. Summary

7.1. Distance variation of the Rods

The resonance length for the spherical and rectangular rod shows a red-shift with decreasing distance. Differences can be seen however, in the increase of the resonance length. The spherical rod has lower resonance lengths at larger distances compared to the rectangular rod. But the increase is larger.

7.2. Calculating the expansion coefficients

In both cases the dipole mode was the most dominant in the expansion. At the largest distance the dipole and quadrupole mode were the first non vanishing terms in both cases. Differences can be seen in higher orders. At smaller distances, first and third order terms are present. This causes the dipole and quadrupole mode to decrease in value of the modulus. The first and third order terms decrease with increasing distance.

A. Code for finding resonance frequencies (spherical caps)

```
% DEMOCOEFFS for spherical

% options for BEM simulation
op = bemoptions( 'sim', 'stat', 'waitbar', 0, 'interp', 'curv' );

% gap distance
gap = 2 : 25;

% dimensions of nanorod
diameter = 10;
height = 40;

% nanorod and gap distance for rectangular rod
p_r = trirod( diameter, height, [ 10, 10, 20 ] );

% number of eigenvalues and boundary elements of first rod
nev = 40;

% allocate expansion coefficients
c1_r = zeros( 1, nev );
c_r = zeros( length(gap), nev);

%% start with others
for ngap = 1 : length(gap)

    % nanorod and gap distance for rectangular rod
    p_r = trirod( diameter, height, [ 10, 10, 20 ] );

    % coupled rectangular rods
    p1_r = shift( p_r, [ 0, 0, - 0.5 * ( height + gap(ngap) ) ] );
% 1st rod
    p2_r = shift( p_r, [ 0, 0,   0.5 * ( height + gap(ngap) ) ] );
% 2nd rod

     % initialize rectangular rods
    p_r = comparticle( epstab, { p1_r, p2_r }, [ 2, 1; 2, 1 ], 1, 2, op );

    % set up BEM solver
    bem_r = bemsolver( p_r, op );
```

```
    % plane wave excitation
    exc = planewave( [ 0, 0, 1 ], [ 1, 0, 0 ], op );

    % eigenmodes for single rod
    pp = comparticle( epstab, { p1_r }, [ 2, 1 ], 1, op );

    [~, ~, ul1_r ] = plasmonmode( pp, nev );

    % resonance wavelength
    enei = max_wave _r(ngap);

    % surface charge
    sig_r = bem_r \ exc( p_r, enei );

    % eigenmodes for single rod
    pp = comparticle( epstab, { p1_r }, [ 2, 1 ], 1, op );

    % loop over eigenmodes
    for iev = 1 : nev
        % coefficients
        c1_r( iev ) = sum( ul1_r ( iev, : ) .' .* sig_r.sig( 1 : p1_r.n )

    end

    c_r(ngap, :) = abs(c1_r);  % / sum_norm;  % sum( abs( c1_r ) );

end

% normalize
c_r = c_r / sum(c_r(1,:));

%% plot coefficients
% plot( abs ( c1_r ) / sum( abs( c1_r ) ), 'o-' );  hold on

% plotting both
figure
imagesc( 1 : nev, gap, abs(c_r) )
% abs(c1_r)
colorbar
title(['Coefficiants for spherical rods with ', num2str(nev), ' coefficient
ylabel('gap distance')
xlabel('number of states')

%%
```

```
figure
semilogy( gap, abs( c_r(:,2) ), '*', 'MarkerSize', 10 )
hold on
semilogy( gap, abs( c_s(:,2) ), '*', 'MarkerSize', 10 )
grid on
title(' Absolute value of the coefficiants for dipole mode as function of
xlabel(' d / nm ', 'FontSize', 14 )
ylabel(' |c| ', 'FontSize', 14 )
set( gca, 'LineWidth', 1.2)
```

B. Code for finding resonance frequencies (rectangular caps)

```
%% initialization

gap = 2:25;
max_wave_s = zeros( 1 , length(gap) );
max_wave_r = zeros( 1 , length(gap) );

% light wavelength in vacuum
enei = linspace( 400, 900, 100 );

xx = linspace(400,900,1000);
% options for BEM simulation
op = bemoptions( 'sim', 'stat',...
                              'waitbar', 0, 'interp', 'curv' );

% plane wave excitation with polarisation
exc = planewave( [ 0, 0, 1; 1, 0, 0 ], op );

% table of dielectric functions
epstab = { epsconst( 1 ), epstable( 'gold.dat' ) };
% dimensions of nanorod
diameter = 10;
height = 40;

for n = 1: length(gap)
% nanorod and gap distance for spherical rod
p_s = trirod( diameter, height, [ 10, 10, 20 ] );

% scale endcap for spherical rod
z = 0.5 * ( height - diameter );
p_s.verts( p_s.verts( :, 3 ) > z, 3 ) = z + ...
( p_s.verts( p_s.verts( :, 3 ) > z, 3 ) - z ) * 0.2;
p_s = particle( p_s.verts, p_s.faces );
p1_s = shift(       p_s,       [ 0, 0, -( max( p_s.pos( :, 3 ) ) + 0.5 * g
p2_s = shift( flip( p_s, 3 ), [ 0, 0,   ( max( p_s.pos( :, 3 ) ) + 0.5 * g

p_s = comparticle( epstab, { p1_s, p2_s },...
                                  [ 2, 1; 2, 1 ], 1, 2, op );

bem_s = bemsolver( p_s, op );
```

```
sca_s = zeros( length( enei ), 2 );


multiWaitbar( 'BEM solver', 0,...
                          'Color', 'g', 'CanCancel', 'on' );

%  loop over wavelengths
    for ien = 1 : length( enei )

    %  surface charge / normalized for incident wave (?)
     sig_s = bem_s \ exc( p_s, enei( ien ) );

     %  scattering and extinction cross sections
     sca_s( ien, : ) = exc.sca( sig_s );

    multiWaitbar( 'BEM solver', ien / numel( enei ) );
    end

%  close waitbar
multiWaitbar( 'CloseAll' );

yy_s = spline( enei, sca_s(:,2)', xx);


[~,max_ind_s] = max( yy_s);
max_wave_s (n) = xx(max_ind_s);

end
%%  plot together
plot( gap, max_wave_s,'*',gap, max_wave_r,'o')
xlabel('gap distance / nm')
ylabel('\lambda / nm')
legend('spherical rod', 'rectangular rod')
grid on
```

C. Calculating coefficients for rectangular rods

```
% DEMOCOEFFS for rectangular

% options for BEM simulation
op = bemoptions( 'sim', 'stat', 'waitbar', 0, 'interp', 'curv' );

% gap distance
gap = 2 : 25;

% dimensions of nanorod
diameter = 10;
height = 40;

% nanorod and gap distance for rectangular rod
p_s = trirod( diameter, height, [ 10, 10, 20 ] );

% number of eigenvalues and boundary elements of first rod
nev = 40;

% allocate expansion coefficients
c1_s = zeros( 1, nev );
c_s  = zeros( length(gap), nev);


%% start with others
for ngap = 1 : length(gap)

    % nanorod and gap distance for rectangular rod
    p_s = trirod( diameter, height, [ 10, 10, 20 ] );

    % coupled rectangular rods
    p1_s = shift( p_s, [ 0, 0, - 0.5 * ( height + gap(ngap) ) ] );
% 1st rod
    p2_s = shift( p_s, [ 0, 0,   0.5 * ( height + gap(ngap) ) ] );
% 2nd rod

    % scale endcap for spherical rod
    z = 0.5 * ( height - diameter );
    p_s.verts( p_s.verts( :, 3 ) > z, 3 ) = z +  ...
        ( p_s.verts( p_s.verts( :, 3 ) > z, 3 ) - z ) * 0.2;
    p_s = particle( p_s.verts, p_s.faces );
    p1_s = shift(       p_s,       [ 0, 0, - ( max( p_s.pos( :, 3 ) ) + 0.5
```

```
    p2_s = shift( flip( p_s, 3 ), [ 0, 0,   ( max( p_s.pos( :, 3 ) ) + 0.5


     % initialize rectangular rods
    p_s = comparticle( epstab, { p1_s, p2_s }, [ 2, 1; 2, 1 ], 1, 2, op );

    % set up BEM solver
    bem_s = bemsolver( p_s, op );

    % plane wave excitation
    exc = planewave( [ 0, 0, 1 ], [ 1, 0, 0 ], op );


    % eigenmodes for single rod
    pp = comparticle( epstab, { p1_s }, [ 2, 1 ], 1, op );

    [~, ~, ul1_s ] = plasmonmode( pp, nev );

    % resonance wavelength
    enei = max_wave_s(ngap);

    % surface charge
    sig_s = bem_s \ exc( p_s, enei );

    % eigenmodes for single rod
    pp = comparticle( epstab, { p1_s }, [ 2, 1 ], 1, op );

    % loop over eigenmodes
    for iev = 1 : nev
        % coefficients
        c1_s( iev ) = sum( ul1_s( iev, : ) .' .* sig_s.sig( 1 : p1_s.n ) .*

    end

    c_s(ngap, :) = c1_s / sum( abs(c1_s)  );

end
```

D. Calculating coefficients for spherical rods

```
% DEMOCOEFFS for spherical

% options for BEM simulation
op = bemoptions( 'sim', 'stat', 'waitbar', 0, 'interp', 'curv' );

% gap distance
gap = 2 : 25;

% dimensions of nanorod
diameter = 10;
height = 40;

% nanorod and gap distance for rectangular rod
p_r = trirod( diameter, height, [ 10, 10, 20 ] );

% number of eigenvalues and boundary elements of first rod
nev = 40;

% allocate expansion coefficients
c1_r = zeros( 1, nev );
c_r = zeros( length(gap), nev);

%% start with others
for ngap = 1 : length(gap)

    % nanorod and gap distance for rectangular rod
    p_r = trirod( diameter, height, [ 10, 10, 20 ] );

    % coupled rectangular rods
    p1_r = shift( p_r, [ 0, 0, - 0.5 * ( height + gap(ngap) ) ] );
% 1st rod
    p2_r = shift( p_r, [ 0, 0,   0.5 * ( height + gap(ngap) ) ] );
% 2nd rod

     % initialize rectangular rods
    p_r = comparticle( epstab, { p1_r, p2_r }, [ 2, 1; 2, 1 ], 1, 2, op );

    % set up BEM solver
    bem_r = bemsolver( p_r, op );

    % plane wave excitation
```

```
    exc = planewave( [ 0, 0, 1 ], [ 1, 0, 0 ], op );

    %  eigenmodes for single rod
    pp = comparticle( epstab, { p1_r }, [ 2, 1 ], 1, op );

    [~, ~, ul1_r ] = plasmonmode( pp, nev );

    %  resonance wavelength
    enei = max_wave _r(ngap);

    % surface charge
    sig_r = bem_r \ exc( p_r, enei );

    %  eigenmodes for single rod
    pp = comparticle( epstab, { p1_r }, [ 2, 1 ], 1, op );

    %  loop over eigenmodes
    for iev = 1 : nev
        %  coefficients
        c1_r( iev ) = sum( ul1_r ( iev, : ) .' .* sig_r.sig( 1 : p1_r.n )

    end

    c_r(ngap, :) = abs(c1_r);  % / sum_norm;  % sum( abs( c1_r ) );

end

% normalize
c_r = c_r / sum(c_r(1,:));

%%  plot coefficients
% plot( abs ( c1_r ) / sum( abs( c1_r ) ), 'o-' );  hold on

% plotting both
figure
imagesc( 1 : nev, gap, abs(c_r) )
% abs(c1_r)
colorbar
title(['Coefficiants for spherical rods with ', num2str(nev), ' coefficient
ylabel('gap distance')
xlabel('number of states')

%%
figure
```

```
semilogy( gap, abs( c_r(:,2) ), '*', 'MarkerSize', 10 )
hold on
semilogy( gap, abs( c_s(:,2) ), '*', 'MarkerSize', 10 )
grid on
title(' Absolute value of the coefficiants for dipole mode as function of
xlabel(' d / nm ', 'FontSize', 14 )
ylabel(' |c| ', 'FontSize', 14 )
set( gca, 'LineWidth', 1.2)
```

Literature

[1] Jeremy J. et al. Baumberg. "Extreme nanophotonics from ultrathin metallic gaps". In: *Nature Materials* 18 (Juli 2019), S. 668–678.

[2] T. Bozhevolnyi S.I & Sondergaard. "General properties of slow-plasmon resonant nanostructures: nano-antennas and resonators". In: *Opt. Express* (2007).

[3] Ruben et. al. Esteban. "The Morphology of Narrow Gaps Modifies the Plasmonic Response". In: *ACS Photonics* (2015), S. 295–305. DOI: 10.1021\ph5004016.

[4] Ulrich Hohenester. *Nano Optics and Plasmonics Theoretical conscepts*. Springer, Aug. 2018.

[5] Ulrich Hohenester und Andreas Trügler. "MNPBEM- A Matlab toolbox for the simulation of plasmonic nanoparticles". In: *Elsevier* (2011). URL: http://physik.uni-graz.at/~uxh/Publications/mnpbem11.pdf.

[6] Q. Li und Z Zhang. "Bonding and Anti-bonding Modes of Plasmon Coupling effects in TiO2-Ag Core-shell Dimers". In: *Sci. Rep.* (2016). DOI: 10.1038.